A new mechanism for increasing density peaking in tokamaks: Improvement of the inward particle pinch with edge ExB shearing

J. Garcia,[1] H. Doerk,[2] T. Görler,[2] and and JET Contributors[3]

[1] *CEA, IRFM, F-13108 Saint-Paul-lez-Durance, France*

[2] *Max-Planck-Institut für Plasmaphysik, Boltzmannstraße 2, D-85748 Garching, Germany*

[3] *See the author list of X Litaudon et al. 2017 Nucl. Fusion 57 102001*

(Dated: November 11, 2018)

Developing successful tokamak operation scenarios, as well as confident extrapolation of present-day knowledge requires a rigorous understanding of plasma turbulence, which largely determines the quality of the confinement. In particular, accurate particle transport predictions are essential due to the strong dependence of fusion power or bootstrap current on the particle density details. Here, gyrokinetic turbulence simulations are performed with physics inputs taken from a JET power scan, for which a relatively weak degradation of energy confinement and a significant density peaking is obtained with increasing input power. This way physics parameters that lead to such increase in the density peaking shall be elucidated. While well-known candidates such as the collisionality are also recovered in this study, it is furthermore found that edge ExB shearing may adopt a crucial role by enhancing the inward pinch. These results may indicate that a plasma with rotational shear could develop a stronger density peaking as compared to a non-rotating one, because its inward convection is increased compared to the outward diffusive particle flux as long as this rotation has a significant on ExB flow shear stabilisation. The possibly significant implications for future devices, which will exhibit much less torque compared to present day experiments, are discussed.

I. INTRODUCTION

In magnetic confinement fusion experiments, highly complex and nonlinear plasma turbulence determines the dominant fraction of cross-field heat, particles, and momentum transport. The performance of future fusion devices, for instance in terms of the confinement time, or the fusion power, are often estimated by means of empirical scaling laws. However, interplays between parameters like the local normalised pressure β, the collisionality, the safety factor q, or sheared ExB flow are known. Designing new promising operation scenarios as well as confidently extrapolating present-day knowledge to future devices thus requires a rigorous understanding of the underlying physics.

Significant advances have been achieved in recent years, many of them obtained through ab-initio gyrokinetic simulations and mainly addressing the heat transport as subject of interest. The significant suppression of Ion Temperature Gradient (ITG) dominated plasma turbulence via electromagnetic fluctuations and fast ions [1, 2], for instance, has opened up the scope of turbulence reduction by alternative mechanisms to the well-known ExB shearing. Such effects have also been shown to play an important role in the so-called isotope effect [3, 4].

However, particle transport has received much less attention in ab-initio gyrokinetic simulations. This is a significant drawback given that in comparison to the temperature profile, the density profile seems to be more affected by the turbulence regime. The reason is the possible existence of a particle pinch due to transport convection which can produce peaked or hollow density profiles, even if the net heat flux is outwards. This has been extensively studied in the framework of the linear or quasi-linear gyrokinetic theory [5–10] as well as from the experimental point of view [11–14]. In particular, the dependence of the pinch, outward or inward, on the turbulence regime, Trapped Electron Modes (TEM) or ITG and its dependence on other physical parameters, such as collisionality, has been highlighted as one of the main reasons for the change of density peaking in different plasma regimes. However, the question whether the physical mechanisms reducing heat transport, in particular those recently discovered, play a similar role in particle transport or particle pinch, still remains. The answer to this question is essential as accurate particle transport understanding and predictions are required since fusion power or bootstrap current, whose contribution are crucial for the future tokamak reactor, enormously depend on them.

In order to analyse what physical mechanisms play a role on particle confinement, and particularly on density peaking, JET discharges with a relatively weak energy confinement degradation and increased density peaking (at constant line-averaged density) with input power [15] have been chosen for analysis. This work extends a previous study [16] with the gyrokinetic turbulence GENE [17], which was mainly focused on heat transport in the inner plasma region, by covering outer radial positions as well as adding the analysis of particle transport including pinch effects. It is often concluded from experiment and quasilinear models that a particle pinch exists, however,

non-linear gyrokinetic simulations covering both the inner and outer part the of the core plasma are still missing. The paper is organised as follows: the modelling set-up is discussed in section II, heat particle at two radial locations is studied in section III, a review of previous particle transport analyses is given in section IV, a first analysis of particle transport is done in section V whereas the new interplay between inward particle pinch and ExB is shown in section VI. In section VII the conclusions are given.

II. SIMULATION SETUP

Two discharges are selected for the analysis of the JET-ILW power scan: 84798 at 6MW NBI power and 84792 at 13MW NBI power. For each of these, an interpretative power balance analysis with experimental data as input has been performed with the CRONOS suite of codes [18]. This allows to determine the NBI power deposition profiles, the magnetic geometry, as well as the power balance turbulent heat fluxes Q_s and particle fluxes Γ_s, which are consistent with the calculated source profiles of each species s. The fluxes are averaged over a sufficient time window $t = 45.2$s-45.45s at a given flux surface. In a second step, these fluxes are compared with the ones obtained from nonlinear GENE simulations. The work at hand extends previous studies documented in Ref. [16] by the analysis of particle transport and density peaking. Furthermore, GENE simulations at the radial position $\rho_{\rm tor} = 0.65$ (outer core) are added to 0.33 (inner core) results. We make use of the local (flux-tube) version of GENE, taking up to three plasma species (electrons and thermal + NBI fast ions) into account. Dedicated tests have demonstrated that adding impurity species (C, Be, W) only marginally affects the results. At least $\{192, 96, 24, 32, 12\}$ grid cells in $\{x, y, z, v_\parallel, \mu\}$ phase space are employed in the nonlinear GENE simulations and numerical convergence tests have been performed in all dimensions for selected runs.

For gaining insights into relevant physics in these inner and outer core cases, parameters are varied around the experimental operation point. The nominal parameters (Tab. I) are extracted from interpretative CRONOS simulations. Some choices made in this procedure are detailed in the following. In Ref. [16], a q-profile sensitivity study has been performed, considering magnetic equilibria with $q = 1.24$ and $q = 0.92$ at $\rho_{\rm tor} = 0.33$, respectively. Here, only the $q = 0.92$ equilibrium which is more consistent with MSE measurements is taken into account. For the discharge 84798, $T_i = T_e$ is assumed due to the uncertainties on the charge exchange (CX) ion temperature measurement which lead to Ti<Te. With this assumption, the total energy content is well fitted within the interpretative CRONOS analysis. Even though also the high power discharge 84792 suffers from error bars on the ion temperature, we decide to use the T_i measurements. Uncertainties exist also in the plasma rotation and the rate of flow shear, to which the turbulence level is very sensitive, particularly at outer radii. In any case, the sensitivity of the results obtained in the following sections to these parameters will be analysed by performing corresponding scans.

	$\rho = 0.33$		$\rho = 0.65$	
	6MW	13MW	6MW	13MW
$\nu_i^\star$	0.04	0.01	0.09	0.02
$1/\rho^\star$	300.72	242.41	432.69	343.07
β_e[%]	1.26	2.00	0.50	0.74
q	0.98	0.92	1.67	1.55
$\hat{s}$	0.30	0.18	1.45	1.71
R/m	3.00	3.03	3.00	3.03
$\alpha_{\rm MHD}$	0.13	0.27	0.24	0.35
$\gamma_{E\times B}/(c_s/R)$	0.19	0.23	0.36	0.53
$Z_{\rm eff}$	1.16	1.26	1.16	1.31
T_{0e}/keV	2.08	3.17	1.01	1.58
$n_{0e}/{\rm m}^3$	4.37	4.35	3.59	3.21
R/L_{Ti}	4.53	5.65	6.21	5.65
R/L_{Te}	4.53	4.07	6.21	5.59
R/L_{ne}	0.69	1.54	2.50	3.44
$\langle Q_i V'\rangle$/MW	1.02	2.86	2.36	5.99
$\langle Q_e V'\rangle$/MW	0.49	1.40	1.60	4.47

Table I. Local parameters obtained from CRONOS for the 6 and 13MW NBI power depositions in the JET power scan at low triangularity δ. A finer reevaluation of the CRONOS interpretative simulations was performed compared to Ref. [16].

III. GENE RESULTS AND POWER BALANCE

In Ref. [16] it was shown that at $\rho_{\rm tor} = 0.33$, both discharges are in the ion temperature gradient (ITG) driven regime, in which electromagnetic stabilisation plays a significant role at high heating power. Extending this study to the more outward radial position $\rho_{\rm tor} = 0.65$, we find microinstabilities rotating in the ion diamagnetic direction as well, as depicted in Fig. 1(a) for the 13MW discharge. The ratio of particle to quasi-linear heat flux $\Gamma_e T_e/Q$ is larger than in the experiment over the full unstable k_y wavenumber range. It is found that Density Gradient Trapped Electron Modes (DGTEM) highly contribute to the mode

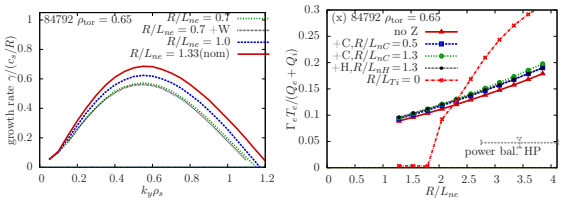

Figure 1. Growth rate spectra (a) and (b) the flux ratio at $k_y\rho_s = 0.33$ as function of R/L_{ne} for various gradient variations of the 13MW discharge at $\rho = 0.65$. The scans reveal a DGTEM contribution to both mode growth and quasilinear particle flux.

as in R/L_{ne} scans at artificially suppressed ITG drive $R/L_{Ti} = 0$, we find a transition from Micro Tearing Modes (MTM) to DGTEM below the experimental value of R/L_{ne}. The DGTEM is characterised by strong R/L_{ne} drive, propagation in electron diamagnetic direction and strong outward particle flux, as depicted in Fig. 1(b). Therefore, this plasma is found in an ITG+TEM regime due to the relatively high density peaking or gradient, respectively. The reliable determination of density gradients in experiments is therefore essential for a correct flux evaluation. Considering impurities (Hydrogen, Carbon, or Beryllium) with $Z_{\text{eff}} \lesssim 1.3$ and various density gradients can somewhat change the growth rates, but the ratio $\Gamma_e T_e/Q$ is not affected.

The power through a given flux surface $\langle Q_s \rangle V'$ as obtained from CRONOS roughly increases proportional to the input power, as can be seen in Fig. 2. Assuming a Gyro-Bohm-like turbulent transport scaling $Q \sim Q_{gB} = c_s p_e (\rho_s/R)^2\ T^{5/2}$, doubling the input power would result in $2^{2/5} = 1.3$ higher temperature and almost unchanged logarithmic temperature gradient $R/L_T = -R\nabla T/T$ if the transport stiffness is preserved. Here, the sound velocity $c_s = (T_e/m_D)^{1/2}$ and the gyroradius $\rho_s = c_s\Omega_i$ are defined, with cyclotron frequency $\Omega_i = m_D c/(eB_0)$ and p_e denotes the electron pressure. However, in the present scan, the temperature increases by a significantly larger factor and appears to be more peaked in the core, see Refs. [15, 16]. This implies that the flux-gradient relation $Q(R/L_T)$ is modified by additional physics, such as electromagnetic (β-) effects, equilibrium $E \times B$ flow shear, increased T_i/T_e, or the presence of fast ions. In the present set of JET experiments, all of the mentioned effects simultaneously increase with NBI beam power. Theoretical analysis is desirable to disentangle their impact, and thus establish more confident extrapolations to higher heating power and future devices, in which the relation between relevant parameters will be different.

As depicted in Fig 2 and Fig 3, the CRONOS heat fluxes can be largely matched by GENE within the error bars of the logarithmic ion temperature gradient R/L_{Ti} which represents the main driving gradient at both radial positions. However, the ratio of the particle-to-heat-flux $\Gamma_e T_e/Q$ is found to be significantly larger in GENE than in CRONOS, especially at the outer radial position. The trend of higher $\Gamma_e T_e/Q$ at higher power is captured, though. Interestingly, the ratio $\Gamma_e T_e/Q$ decreases with R/L_T for both discharges showing that the thermodiffusion pinch might be negative. This will be further discussed in section V. Generally, the discrepancies between GENE and CRONOS may be due to input uncertainties. The fact that such discrepancies increase towards the edge may be evidence for associated uncertainties in the evaluation of the interpreted particle flux in that region. The latter may be less accurate if particle sources or sinks – for instance, by means of gas injection or Edge Localized Modes (ELMs) – play a role at outer radial position but are not considered in the CRONOS simulations. This will be analysed in the future. Before further parameter scans in linear and nonlinear simulations are presented in Sec. V, it is useful to briefly review the present knowledge concerning particle fluxes in fusion plasmas.

IV. PARTICLE FLUX IN GYROKINETICS

A rather complete overview in this context is given by Angioni and co-workers, [6–9] who showed the strong impact of collisionality on the particle flux through a change of the particle pinch. Most of the previous studies have, however, been performed in the electrostatic limit ($\beta \to 0$). Also more recent nonlinear simulation work falls into this regime [19]. An early extension to the electromagnetic regime is presented in Ref. [20], where increased particle flux due to larger β is found. This effect can be mainly related to the non-adiabaticity of passing electrons and it is partially balanced by considering a self-consistent equilibrium pressure gradient (α_{MHD}). The above reference furthermore confirms the validity of the collisionality dependence of the ITG caused outward particle flux in the electromagnetic regime. However, the direct applicability of such studies to NBI heated plasmas is difficult as as higher β is obtained with simultaneously increased particle source, which is known to play a role on the density peaking [14, 21–24] and that may counteract β-enhanced fluxes. Additionally, the NBI tend to increase the torque and plasma rotation which can have significant impact on the shearing flows which, at least in the ITG/TEM mixed turbulence regime, sheared flows can indirectly change the balance between those

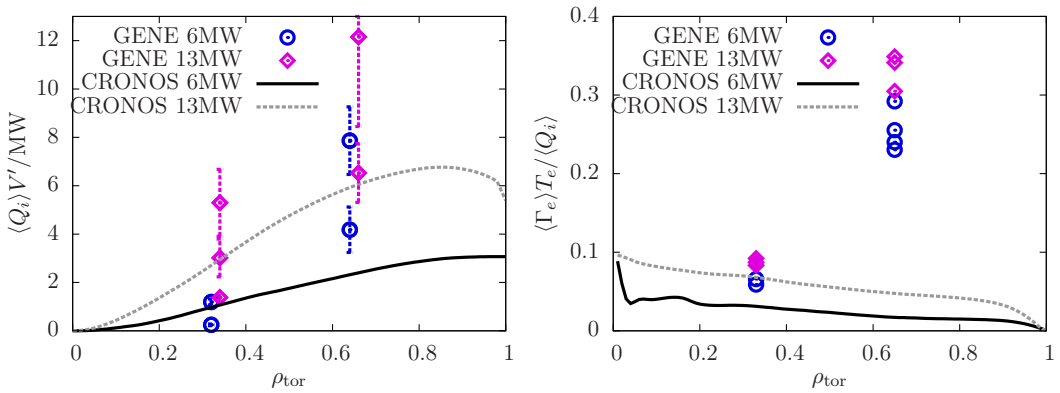

Figure 2. (a) Power balance is matched by GENE simulations (data from R/L_{Ti} scans of Fig. 3). (b) In the same GENE simulations, $\Gamma_e T_e/Q_i$ has larger values than CRONOS, especially in outer radial positions.

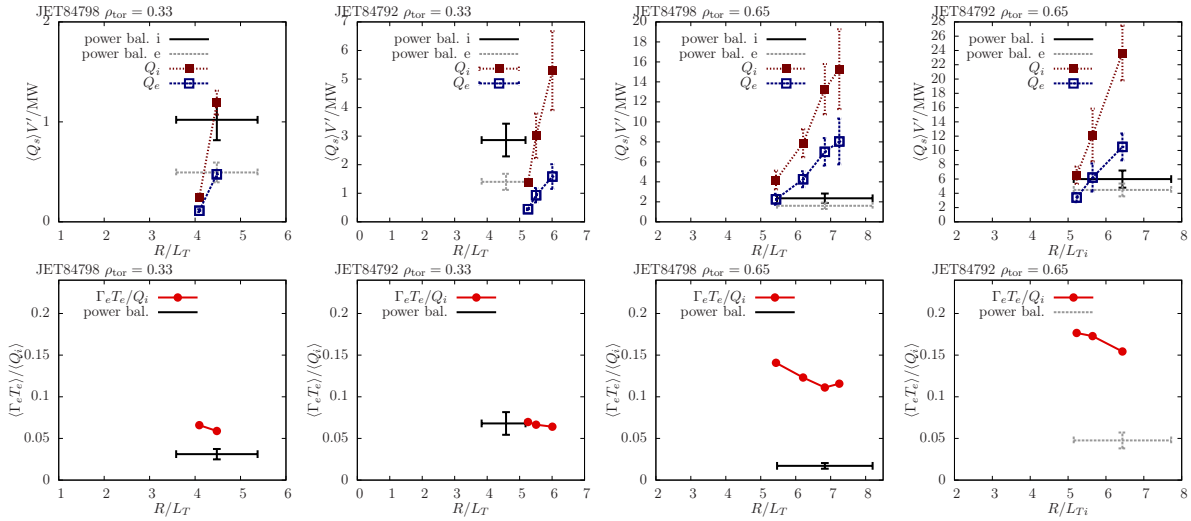

Figure 3. Same simulation data as in Fig: 2: R/L_{Ti} scans for 6MW and 13 MW discharges at two radial positions.

two types of turbulence, since they more strongly affect ion modes. The direct impact of the rotation terms on the particle flux has been studied in Ref. [25, 26]. In an ITG example, Deuterium particle transport is found to be dominated by the convective flux (C_p), which is hardly affected by plasma rotation. The roto-diffusion coefficient (C_u) is small and inward. However, the dependence of the particle flux on flow shear has not been intensively studied, partially because it is not easily accessible with the quasi-linear approach. Such analysis is specially important in highly electromagnetic regimes as the aforementioned JET power scan in order to disentangle the impact of different effects collinear with NBI heating.

V. PARAMETER SCANS IN NONLINEAR SIMULATIONS

In the following, we perform nonlinear parameters scans to assess the scaling of turbulent transport with focus on the 13MW high power discharge with high density peaking. In line with expectation, lower collisionality and reduced density gradient are found to yield lower $\Gamma_e T_e/Q_{i,e}$. Off-diagonal terms play a role as well: thermodiffusion tends to be inward as could already be concluded from the R/L_{Ti} scans in Fig. 3. Increased β has no significant impact on $\Gamma_e T_e/Qi, e$, in contrast to the ASDEX Upgrade hybrid case discussed in Ref. [20]. While flow shear is very efficient in quenching the turbulence at outer radii, it has no strong impact on the $\Gamma_e T_e/Q_{i,e}$ ratio at $\rho_{\rm tor} = 0.65$. However, its impact is significantly increased at outer radii as will be demonstrated for $\rho_{\rm tor} = 0.75$ where a

strong pinch reversal is observed.

A. Collisionality scans

Reaching lower collisionality can strongly increase the turbulence level and somewhat lower the $\Gamma_e T_e/Q_i$ flux ratio, as can be seen in Fig. 4. In the 13MW discharge the collisionality is about a factor of two lower than in the 6MW discharge. When multiplying the collisionality by a factor of two with otherwise 13MW at $\rho_{\rm tor} = 0.65$ parameters will completely suppress turbulence, because the stabilising factors β and $\gamma_{E\times B}$ are stronger than in the low power case. In the other limit of $\nu_{ei} = 0$, $\Gamma_e T_e/Q_i$ is about 25% smaller at $\rho_{\rm tor} = 0.65$ and more than 50% at the inner radial positions. In these nonlinear simulations, the transport fluxes peak around $k_y \sim 0.35$ ($\rho_{\rm tor} = 0.33$) and $k_y = 0.4$ ($\rho_{\rm tor} = 0.65$) and radially outward particle flux is observed at all considered k_y wavenumbers – regardless of the collision rate. Altogether, the stronger impact of collisionality on particle than on heat transport is recovered here.

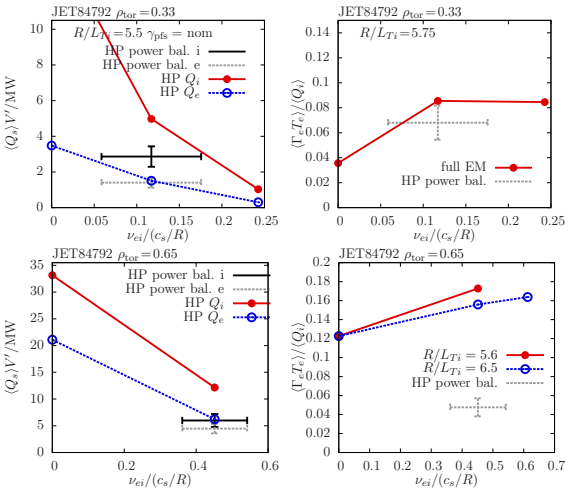

Figure 4. Impact of collisionality on the heat flux and the flux ratio in the 13MW high power discharge at $\rho = 0.33$ ($R/L_{Ti} = 5.5$) and $\rho_{\rm tor} = 0.65$.

B. Electromagnetic effects, β

Regarding the impact of finite β, a strong turbulence stabilisation can be observed at the inner radial position in the high power case while β seems to play a less important role at $\rho_{\rm tor} = 0.65$. The linear simulations shown in Fig. 5 confirm the expected increase of $\Gamma_e T_e/Q_i$. In the nonlinear simulations, however, the reduction of the overall turbulence level is found, but $\Gamma_e T_e/Q_i$ remains basically unchanged.

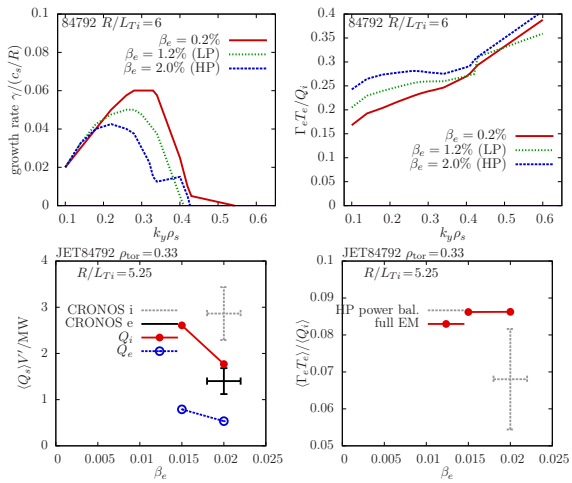

Figure 5. Impact of beta on (a) linear growth rate, (b) quasilinear ratio $\Gamma_e T_e/Q_i$, (c) nonlinear heat flux and (d) flux ratio for the 13MW discharge at $\rho = 0.33$, fixing $R/L_{Ti} = 5.25$.

C. Density gradient R/L_{ne} variations

Although the heat fluxes at $\rho_{\rm tor} = 0.33$ are found to respond non-monotonically to dedicated scans in the electron density gradient R/L_{ne}, the ratio $\Gamma_e T_e/Q_i$ clearly increases, as can be seen in Fig. 6. The figure furthermore demonstrates a similar behaviour at the $\rho_{\rm tor} = 0.65$ position. Often, the peaking factor is computed by matching the outward flux with the particle source by only scanning R/L_n, without considering other physics input. This procedure would predict a significantly more flat density peaking.

D. Flow shear impact

To our knowledge, no nonlinear gyrokinetic simulations are documented regarding the impact of flow shear on particle confinement. Here, we close this gap by varying $\gamma_{\rm ExB}$ and $\gamma_{\rm pfs}$, the parallel velocity gradient (PVG), in dedicated nonlinear runs for the JET power scan. In Fig. 7, only γ_{ExB} is scanned, keeping $\gamma_{\rm pfs}$ constant. Note that the input coefficients are defined such that $\gamma_{\rm pfs} = \gamma_{E\times B}$ in case of purely toroidal flow, while geometry related factors are multiplied within the code. In the electromagnetic cases at $\rho_{\rm tor} = 0.33$, ExB shear reduces the heat flux only at values somewhat larger than the nominal one. The particle flux per heat flux remains almost unchanged. At $\rho_{\rm tor} = 0.65$ the overall flow shear stabilisation is more pronounced,

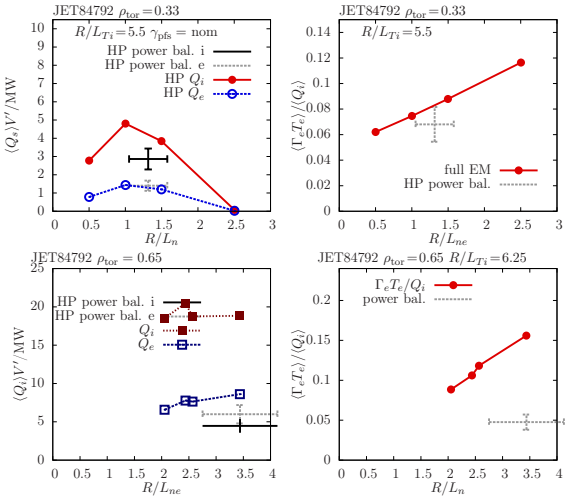

Figure 6. Impact of R/L_{ne} on the heat flux and the flux ratio at $\rho = 0.33$ (($R/L_{Ti} = 5.5$)) and $\rho_{\rm tor} = 0.65$.

in line with previous research [27], but $\Gamma_e T_e/Q_i$ is still not strongly affected (a slight reduction can be noted). For these $\rho = 0.65$ cases, we show also the result for keeping $\gamma_{\rm pfs} = \gamma_{E\times B}$ in the scan, which leads to reduced stabilisation in line with [28], but does not alter $\Gamma_e T_e/Q_i$. However, in order to develop a better idea on the role of ExB on density peaking, a more extended study on its impact on the particle pinch has to be carried out. This will be done in the next section. Additionally, the radial location $\rho = 0.75$ will be considered.

VI. PARTICLE PINCH IN NONLINEAR GYROKINETICS

Some possible indications concerning the impact of ExB on particle transport and density peaking have been suggested both from modeling [23] and experiments [29]. However, so far no clear picture regarding the nature of such process could be drawn. Particle transport can be separated into a diffusive part $\Gamma^D = n\,D\,R/L_n$ and a non-diffusive particle part, Γ^V as

$$\Gamma_e = \Gamma^D + \Gamma^V = n_e D_{ne}\frac{a}{L_{ne}} + n_e V \qquad (1)$$

with $n_e V$ denoting a convective contribution with V the particle pinch. However, the non-diffusive particle part can also have a diffusive contribution from the temperature gradient drive (thermodiffusion). The final flow can be therefore decomposed as

$$\Gamma_e = n_e D_{ne}\frac{a}{L_{ne}} + n_e D_{Te}\frac{a}{L_{Te}} + n_e V \qquad (2)$$

In this paper, an approximation to the ratio of pinch to diffusion is obtained by adding a passive electron species with $a/L_n = 0$, which removes pure particle diffusive transport and yields the particle flux Γ^V. We expect that this approach of determining Γ^V and Γ^D captures the main pinch physics although the coefficients V and D of active electrons would depend on the density gradient to some extent.

In a first step, the particle flux separation as described in Eq. 1 shall now be employed to results at more outer radial positions where ExB shear effects tend to be even more relevant. Fig. 8 displays the dependence of the ratio $\Gamma_e T_e/Q_i$ on the ExB shear at $\rho = 0.75$ in the case of a pure γ_{ExB} scan and in the alternative case with γ_{PVG} accordingly changed with the ExB shearing. Clearly and unlike the case at $\rho = 0.65$ the ExB shearing has a strong effect on the ratio $\Gamma_e T_e/Q_i$ leading to $\Gamma_e T_e/Q_i \sim 0$ for $\gamma_{ExB}/\gamma_{ExB,exp} = 1.4$. Such trend is modulated when the PVG is included, which prevents the full stabilization of the particle flux.

The corresponding diffusive and convective fluxes spectra are analyzed in Fig. 9. For the diffusive part, Γ^D, the ExB shearing acts as expected, shifting the spectrum towards higher $k_y\rho_s$ (and therefore reducing the global transport) compared to the case with no ExB and PVG effects. The cases with only PVG or nominal ExB and PVG are in between these two extreme cases. Compared to this expected behavior, the convective flux Γ^V has some unexpected features. Comparing the cases with no ExB and PVG and the case with only ExB we also observe a shift towards higher $k_y\rho_s$ but this shift is accompanied by a general reversal of the flux, which becomes significantly negative (therefore of inward pinch nature). The effect of PVG is somehow surprising as well as it decreases the inward pinch when added to the simulation with only ExB but it definitely increases such negative pinch when added to the simulation with no effects.

	V(m/s)	RV/χ_i	Γ^V/Γ^D
ExB=0 PVG=0	1.29	0.09	0.12
ExB=0 PVG=nom	-0.49	-0.12	-0.15
ExB=nom PVG=nom	-0.75	-0.24	-0.29
ExB=nom PVG=0	-2.19	-0.42	-0.5

Table II. Non-linear simulation results for different combinations of ExB and PVG values including nominal values (refereed as nom) with χ_i the ion heat diffusivity.

A summary of the changes on Γ^D and Γ^V is presented in Tab. II. The particle pinch becomes strongly inward with increasing ExB shearing. This fact leads to a much stronger impact of

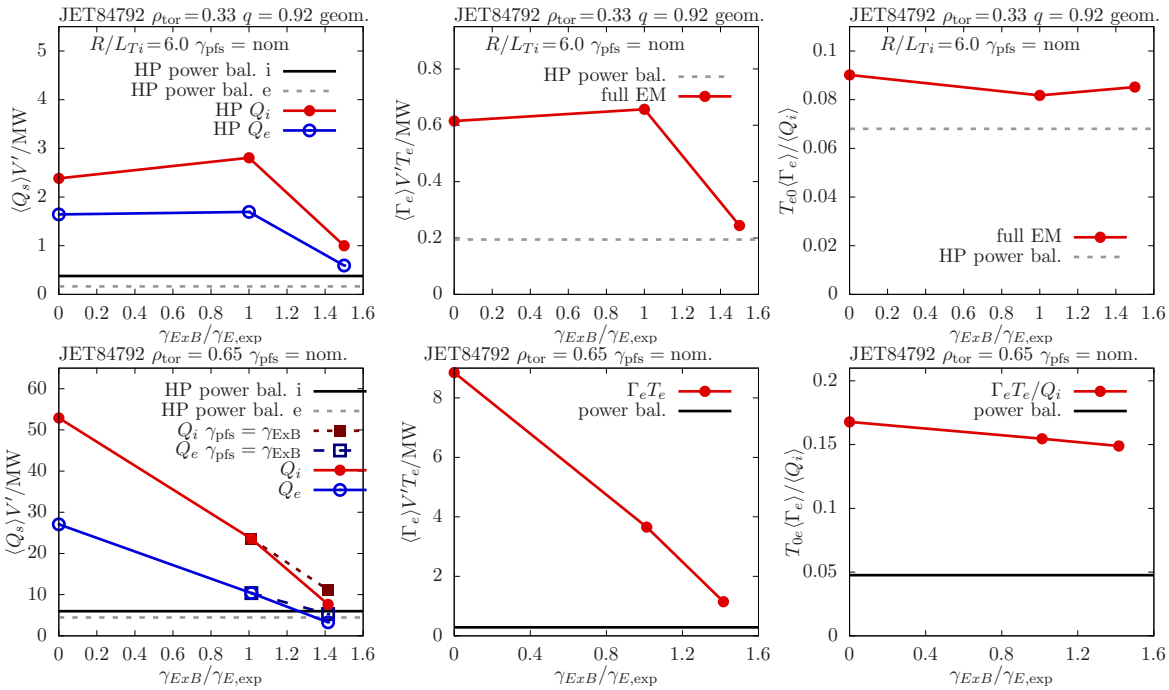

Figure 7. Impact of ExB rotation shear on heat flux (left), particle flux (center), and their ratio (right) for the q = 0.92 geometry at ρ_{tor} = 0.33 (top) and 0.65 (bottom). The CRONOS values are added as black-solid or gray-dashed lines for reference.

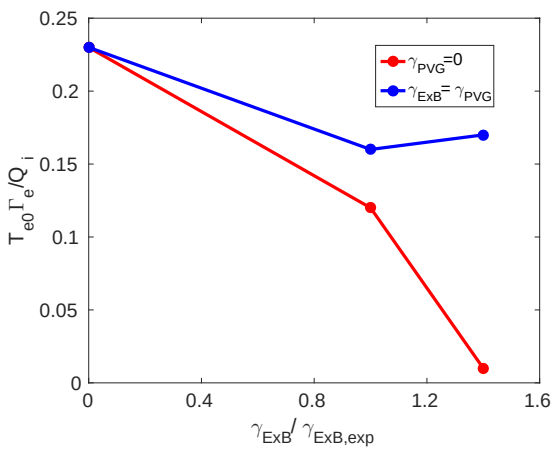

Figure 8. $\Gamma_e T_e/Q_i$ for the case with only ExB shearing $\gamma_{PVG} = 0$ and with equal ExB and PVG shearing $\gamma_{ExB} = \gamma_{PVG}$ at $\rho_{tor} = 0.75$.

ExB shearing on the particle than the heat transport as demonstrated by means of the factor RV/χ_i in Tab. II. The density peaking would indeed benefit from such trend as can be derived from the ratio Γ^V/Γ^D which increases in absolute value and becomes negative from the case without to the case with ExB shearing. The role of PVG is complex as it can be stabilizing or destabilizing depending on the plasma conditions. Nevertheless, in nominal conditions for both ExB and PVG, the pinch is inward and the ratio Γ^V/Γ^D clearly shows that flow shearing plays a role on the increased density peaking obtained in those JET plasmas.

In order to shed light on the origin of the strong inward pinch with ExB shearing an alternative simulation has been performed by removing the thermodiffusion part of the pinch, i.e. by setting $L_{Te} = 0$. The spectra for the cases with and without thermodiffusion contribution for the simulation with solely ExB shear but no PVG are displayed in Fig. 10. Clearly, the strong inward pinch with ExB shearing disappears if thermodiffusion is removed, implying that, as it happens with collisionality, the change of direction of the particle pinch with ExB shearing is also linked to thermodiffusion. This has profound implications on the way experiments could be planned as a way to study the dependence of density peaking with collisionality is to use NBI heating, which in addition to the fuelling leads to an extra collinear effect by increasing the toroidal rotation (the main source of ExB shearing). Decoupling such effects is essential for the extrapolation of present-days tokamak devices to futures ones as ITER, which will have presumably less toroidal rotation due to the weaker NBI torque.

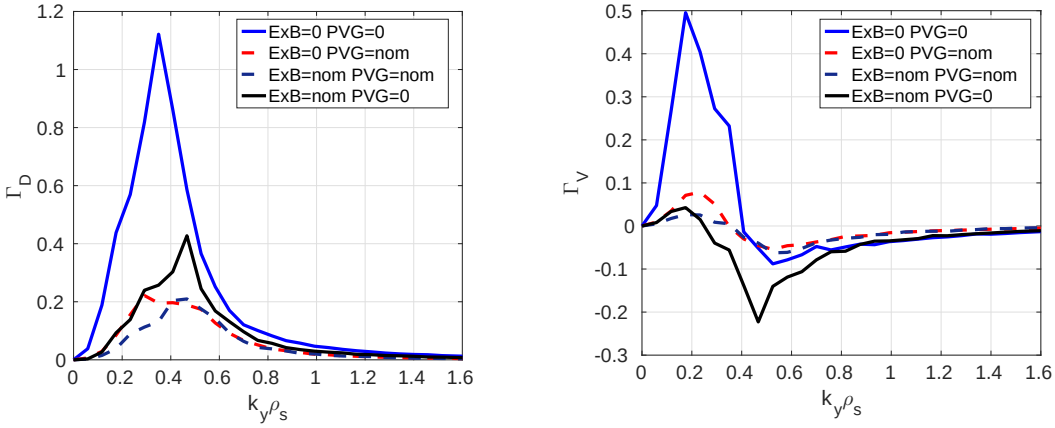

Figure 9. Γ^D and Γ^V spectrum for different combinations of ExB and PVG flow shearing at $\rho_{\rm tor} = 0.75$.

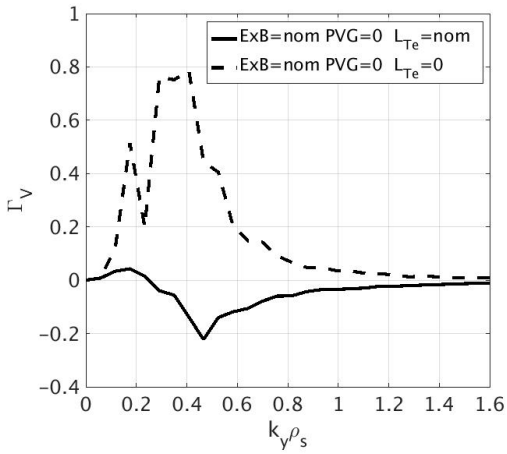

Figure 10. Γ^V spectrum comparison between the case with only nominal ExB shearing and nominal L_{Te} or $L_{Te} = 0$ at $\rho_{\rm tor} = 0.75$.

VII. SUMMARY AND CONCLUSIONS

The particle transport in JET plasmas with a significant increase of density peaking with NBI power has been studied by means of non-linear gyrokinetic simulations.

Linear simulations show that these plasmas are ITG dominated and no transition to TEM is observed when the NBI power is changed although subdominant TEM are present due to the high density peaking. While well established parameters playing a role on particle transport and density peaking could be recovered with the GENE simulations, some new factors have also been identified to be important. In particular, ExB flow shearing can enhance the inward particle pinch leading to a significant decrease of the ratio $\Gamma_e T_e/Q_i$. This effect is stronger at outer radial locations which means that it can be particularly significant close to the pedestal region. Therefore, in the outer part of the plasma, ExB shearing may have a stronger impact on particle than on heat transport.

These findings are further substantiated by an analysis of the ratio Γ^V/Γ^D which demonstrates an enhanced inward pinch with ExB shearing. The latter may, for instance, be found to be significant in the outer part of rotating plasmas and therefore cause visible density peaking in such scenarios. On the other hand, it is also found that PVG can limit the inward pinch generated by the ExB shearing to some degree.

The results shown in this paper may have profound consequences on the way density peaking is understood. Whereas the dependence on collisionality has been highlighted as the main cause for generating a particle pinch, the experimental evidence leading to such conclusion were based in a non-negligible part on NBI-heated plasmas where the NBI can collinearly increase the plasma torque and therefore change the ExB shearing. Therefore, experiments decoupling collisionality and rotation shearing should be encouraged. This could lead as well to the change of some scaling laws used for the extrapolation of present day experiments. This is an essential step towards the proper evaluation of density peaking in future tokamak devices with different plasma conditions.

However some drawbacks have also been encountered in this study. In particular, it remains difficult to match the source balance particle flux in the outer part of the plasma which leads to a overestimation of the ratio $\Gamma_e T_e/Q_i$. This shows that the proper evaluation of the particle sources and sinks in that plasma region is essential.

Further rotating frame effects like centrifugal and coriolis drifts have not been considered here, and may be candidates for some extra missing physics ingredients.

ACKNOWLEDGEMENTS

The authors would like to thank C. Angioni, A. Di Siena, E. Poli, M. J. Pueschel and D. Told for valuable discussions. This work has been carried out within the framework of the EUROfusion Consortium and has received funding from the Euratom research and training programme 2014-2018 under grant agreement No 633053. The views and opinions expressed herein do not necessarily reflect those of the European Commission. The numerical results presented in this work were carried out using the HELIOS supercomputer system at the Computational Simulation Centre of International Fusion Energy Research Centre (IFERC-CSC), Aomori, Japan, under the Broader Approach collaboration between Euratom and Japan, implemented by Fusion for Energy and JAEA, as well as using the resources of the MPCDF computing center, Garching, Germany, the BSC, Barcelona, Spain, under the PRACE project ZONALGENE and the MARCONI supercomputer system at CINECA, Italy.

REFERENCES

[1] J. Citrin, F. Jenko, P. Mantica, D. Told, C. Bourdelle, J. Garcia, J. W. Haverkort, G. M. D. Hogeweij, T. Johnson, and M. J. Pueschel, Phys. Rev. Lett. **111**, 155001 (2013).

[2] J. Garcia, C. Challis, J. Citrin, H. Doerk, G. Giruzzi, T. Görler, F. Jenko, P. Maget, and JET Contributors, Nucl. Fusion **55**, 053007 (2015).

[3] J. Garcia, T. Görler, F. Jenko, and G. Giruzzi, Nuclear Fusion **57**, 014007 (2017).

[4] J. Garcia, T. Görler, and F. Jenko, Physics of Plasmas **25**, 055902 (2018).

[5] C. Bourdelle, Plasma Physics and Controlled Fusion **47**, A317 (2005).

[6] C. Angioni, E. Fable, M. Greenwald, M. Maslov, A. G. Peeters, H. Takenaga, and H. Weisen, Plasma Phys. Controll. Fusion **51**, 124017 (2009).

[7] E. Fable, C. Angioni, and O. Sauter, Plasma Phys. Controll. Fusion **52**, 015007 (2010).

[8] C. Angioni, R. M. McDermott, F. J. Casson, E. Fable, A. Bottino, R. Dux, R. Fischer, Y. Podoba, T. Pütterich, F. Ryter, and E. Viezzer, Phys. Rev. Lett. **107**, 215003 (2011).

[9] C. Angioni, Y. Camenen, F. J. Casson, E. Fable, R. M. McDermott, A. G. Peeters, and J. E. Rice, Nucl. Fusion **52**, 114003 (2012).

[10] M. Romanelli, G. Regnoli, and C. Bourdelle, Physics of Plasmas **14**, 082305 (2007).

[11] G. T. Hoang, C. Bourdelle, B. Pégourié, B. Schunke, J. F. Artaud, J. Bucalossi, F. Clairet, C. Fenzi-Bonizec, X. Garbet, C. Gil, R. Guirlet, F. Imbeaux, J. Lasalle, T. Loarer, C. Lowry, J. M. Travère, and E. Tsitrone (Tore Supra Team), Phys. Rev. Lett. **90**, 155002 (2003).

[12] G. T. Hoang, C. Bourdelle, X. Garbet, J. F. Artaud, V. Basiuk, J. Bucalossi, F. Clairet, C. Fenzi-Bonizec, C. Gil, J. L. Ségui, J. M. Travère, E. Tsitrone, and L. Vermare, Phys. Rev. Lett. **93**, 135003 (2004).

[13] C. Angioni, A. G. Peeters, G. V. Pereverzev, F. Ryter, and G. Tardini (ASDEX Upgrade Team), Phys. Rev. Lett. **90**, 205003 (2003).

[14] H. Weisen, A. Zabolotsky, C. Angioni, I. Furno, X. Garbet, C. Giroud, H. Leggate, P. Mantica, D. Mazon, J. Weiland, L. Zabeo, K.-D. Zastrow, and J.-E. contributors, Nuclear Fusion **45**, L1 (2005).

[15] C. Challis, J. Garcia, M. Beurskens, P. Buratti, E. Delabie, P. Drewelow, L. Frassinetti, C. Giroud, N. Hawkes, J. Hobirk, E. Joffrin, D. Keeling, D. King, C. Maggi, J. Mailloux, C. Marchetto, D. McDonald, I. Nunes, G. Pucella, S. Saarelma, J. Simpson, and JET Contributors, Nucl. Fusion **55**, 053031 (2015).

[16] H. Doerk, C. Challis, J. Citrin, J. Garcia, T. Görler, F. Jenko, and J. Contributors, Plasma Phys. Controll. Fusion **58**, 115005 (2016).

[17] W. Dorland, F. Jenko, M. Kotschenreuther, and B. N. Rogers, Phys. Rev. Lett. **85**, 5579 (2000).

[18] J. Artaud, V. Basiuk, F. Imbeaux, M. Schneider, J. Garcia, G. Giruzzi, P. Huynh, T. Aniel, F. Albajar, J. Ané, A. Bécoulet, C. Bourdelle, A. Casati, L. Colas, J. Decker, R. Dumont, L. Eriksson, X. Garbet, R. Guirlet, P. Hertout, G. Hoang, W. Houlberg, G. Huysmans, E. Joffrin, S. Kim, F. Köchl, J. Lister, X. Litaudon, P. Maget, R. Masset, B. Pégourié, Y. Peysson, P. Thomas, E. Tsitrone, and F. Turco, Nucl. Fusion **50**, 043001 (2010).

[19] D. R. Mikkelsen, M. Bitter, L. Delgado-Aparicio, K. W. Hill, M. Greenwald, N. T. Howard, J. W. Hughes, J. E. Rice, M. L. Reinke, Y. Podpaly, Y. Ma, J. Candy, and R. E. Waltz, Phys. Plasmas **22**, 062301 (2015).

[20] T. Hein, C. Angioni, E. Fable, and J. Candy, Phys. Plasmas **17**, 102309 (2010).

[21] H. Weisen, A. Zabolotsky, M. Maslov, M. Beurskens, C. Giroud, D. Mazon, and J.-E. contributors, Plasma Phys. Controll. Fusion **48**, A457 (2006).

[22] M. Maslov, C. Angioni, H. Weisen, and JET-EFDA contributors, Nucl. Fusion **49**, 075037 (2009).

[23] J. Garcia, N. Hayashi, B. Baiocchi, G. Giruzzi, M. Honda, S. Ide, P. Maget, E. Narita, M. Schneider, H. Urano, and the JT-60U Team, Nuclear Fusion **54**, 093010 (2014).

[24] T. Tala, in *28th IAEA Int. Conf. on Fusion Energy* (2018).

[25] F. J. Casson, A. G. Peeters, C. Angioni, Y. Camenen, W. A. Hornsby, A. P. Snodin, and G. Szepesi, Phys. Plasmas **17**, 102305 (2010).

[26] F. J. Casson, A. G. Peeters, C. Angioni, Y. Camenen, W. A. Hornsby, A. P. Snodin, and G. Szepesi, Phys. Plasmas **19**, 099902 (2012).

[27] J. Citrin, J. Garcia, T. Görler, F. Jenko, P. Mantica, D. Told, C. Bourdelle, D. R. Hatch, G. M. D. Hogeweij, T. Johnson, M. J. Pueschel, and M. Schneider, Plasma Phys. Control. Fusion **57**, 014032 (2015).

[28] J. Citrin, F. Jenko, P. Mantica, D. Told, C. Bourdelle, R. Dumont, J. Garcia, J. W. Haverkort, G. M. D. Hogeweij, T. Johnson, M. J. Pueschel, and J.-E. contributors, Nucl. Fusion **54**, 023008 (2014).

[29] X. Wang, S. Mordijck, L. Zeng, L. Schmitz, T. L. Rhodes, E. J. Doyle, R. Groebner, O. Meneghini, G. M. Staebler, and S. P. Smith, Plasma Physics and Controlled Fusion **58**, 045026 (2016).